Electronic Supplementary Information for Dalton Transactions

Supplementary data

Synthesis and characterization of homo and hetero-valent tetra- hexa- hepta- and decanuclear manganese clusters using pyridyl functionalized *β*-diketone, carboxylate and triethanolamine ligands.

Stuart K. Langley[a], Nicholas F. Chilton[a], Massimiliano Massi[b], Boujemaa Moubaraki[a], Kevin J. Berry[c] and Keith S. Murray[a*]

- **Experimental and Crystallographic information for $3a.2(CH_3)_2CO.2MeOH$, $3b.3CH_2Cl_2.H_2O$ and $4a.2Et_2O.3MeOH.H_2O$.**

$[Mn_7(pppd)_6(tea)(OH)_3][NO_3]_2.\ 2(CH_3)_2CO.2MeOH$ (3a)

The method for **3** was followed but with $Mn(NO_3)_2.4H_2O$ (0.25 g, 1 mmol) used instead of $Mn(BF_4)_2.xH_2O$. Orange/red crystals of **3a** were grown following ether diffusion into a MeCN/acetone solution of product. Yield: 51 mg, 15.1 %. Anal. Calculated (found) for **3a**.$2(CH_3)_2CO.2MeOH$: $Mn_7C_{98}H_{95}O_{28}N_9$: C, 55.75 (55.56); H, 4.29 (4.19); N, 5.65 (5.34). IR data ATR (cm^{-1}): 3235br, 2865w, 1584s, 1555m, 1512s, 1489w, 1465w, 1449s, 1439s, 1413s, 1335m, 1283s, 1225m, 1063w, 1044w, 942w, 767s, 715w, 623w.

$[Mn_7(dppd)_6(tea)(OH)_3][BF_4]_2.3CH_2Cl_2.H_2O$ (3b)

The method for **3** was followed but with 1,3-di(pyridine-2-yl)propane-1,3-dione (0.18 g, 1 mmol) used in place of 1-phenyl-3-(2-pyridyl)propane-1,-dione. Orange/red crystals of **3b** were grown from a CH_2Cl_2 solution that was layered with Et_2O. Yield: 51 mg, 16.2 %. Anal. Calculated (found) for **3b**. : $Mn_7C_{87}H_{77}O_{19}N_{13}Cl_6B_2F_8$: C, 43.91 (43.76); H, 3.26 (3.22); N, 7.65 (7.34). IR data ATR (cm^{-1}): 3235br, 2851m, 1585s, 1494w, 1410s, 1355m, 1310m, 1248w, 1224w, 1065s, 1044s, 944w,768w, 715w, 624w.

$[Mn_7(paa)_6(OMe)_6][ClO_4]_2.2Et_2O.3MeOH.H_2O$ (4a)

The method for **4** was followed but with $Mn(ClO_4)_2.6H_2O$ (0.36 g, 1 mmol) used instead of $Mn(NO_3)_2.4H_2O$. Yield: 170 mg, 58.6 %. Anal. Calculated (found) for

4a.2Et_2O.3MeOH.H_2O : $Mn_7C_{71}H_{106}O_{32}N_{12}Cl_2$: C, 40.70 (40.81); H, 5.10 (5.14); N, 8.02 (8.25). Selected IR data ATR (cm^{-1}): 3339w, 2821w, 1637w, 1591s, 1520m, 1456s, 1412s, 1337s, 1280w, 1261w, 1239w, 1204w, 1159w, 1102w, 1026w, 973w, 773w, 623w.

- Crystal data for **3a**.2$(CH_3)_2CO$.2MeOH : $C_{98}H_{95}N_9O_{28}Mn_7$ (2231.44 g mol-1); triclinic, *a* = 13.638(3), *b* = 14.702(3), *c* = 15.223(3) A°, α = 116.11(3), β = 91.34(3), γ = 90.92(3), *V* = 2738.9(9) A° ^{3}, *T* = 100(2) K, *P-1*, *Z* = 1, μ(Synchrotron) = 0.855 mm-1, *F*(000) = 1142, 2788 reflections with 7099 unique (*R*int = 0.0346), final wR_2 = 0.1629, *S* = 1.077 (all data), R_1 [I ≥ 2s(I)] = 0.0576. CCDC ?????.
- Crystal data for **3b**.3CH_2Cl_2.H_2O : $C_{87}H_{77}N_{13}O_{19}Mn_7Cl_6$ (2379.53 g mol-1); monoclinic, *a* = 14.3254(13), *b* = 25.518(2), *c* = 29.7632(3) A°, β = 99.014(4), *V* = 10745.73(17) A° ^{3}, *T* = 123(2) K, *P21/c*, *Z* = 4, μ(Mo-K) = 1.026 mm-1, *F*(000) = 4784, 75991 reflections with 11236 unique (*R*int = 0.1238), final wR_2 = 0.4813, *S* = 1.050 (all data), R_1 [I ≥ 2s(I)] = 0.157. CCDC ?????.
- Crystal data for **4a**.2Et_2O.3MeOH.H_2O : $C_{71}H_{106}N_{12}O_{32}Mn_7Cl_2$ (2095.15 g mol-1); triclinic, *a* = 13.041(5), *b* = 14.379(2), *c* = 14.732(3) A°, α = 113.236(8), β = 97.854(12), γ = 97.756(12), *V* = 2459.8(11) A° ^{3}, *T* = 123(2) K, *P-1*, *Z* = 1, μ(Mo-K) = 1.002 mm-1, *F*(000) = 1079, 50047 reflections with 11672 unique (*R*int = 0.0344), final wR_2 = 0.2326, *S* = 1.052 (all data), R_1 [I ≥ 2s(I)] = 0.0622. CCDC ?????.

Atoms	Mn(II)	Mn(III)	Mn(IV)
Mn1	3.43	**3.15**	3.10
Mn2	3.35	**3.09**	3.03
Mn3	3.34	**3.11**	3.07
Mn4	4.49	4.15	**4.07**
Mn5	3.48	**3.20**	3.14
Mn6	3.33	**2.97**	2.91
Mn7	3.45	**3.18**	3.11
Mn8	**2.08**	1.93	1.88
Mn9	**2.13**	1.91	1.85
Mn10	**2.18**	2.01	1.95

Table S1. Bond valence sum calculations for **1**. The oxidation state for each metal is the whole number closest to the value in bold.

Atoms	Mn(II)	Mn(III)	Mn(IV)
Mn1	**2.18**	1.99	1.93
Mn2	**2.11**	1.93	1.87
Mn3	**1.70**	1.59	1.54

Table S2. Bond valence sum calculations for **2**. The oxidation state for each metal is the whole number closest to the value in bold.

Atoms	Mn(II)	Mn(III)	Mn(IV)
Mn1	**1.85**	1.72	1.68
Mn2	**2.18**	2.01	1.93
Mn3	**2.13**	1.96	1.90
Mn4	**2.14**	1.97	1.91
Mn2’	**2.12**	1.95	1.87
Mn3’	**2.12**	1.95	1.89
Mn4’	**2.05**	1.88	1.82

Table S3. Bond valence sum calculations for **3**. The oxidation state for each metal is the whole number closest to the value in bold.

Atoms	Mn(II)	Mn(III)	Mn(IV)
Mn1	**2.15**	2.00	1.93
Mn2	**1.88**	1.74	1.70

Table S4. Bond valence sum calculations for **4**. The oxidation state for each metal is the whole number closest to the value in bold.

Atoms	Mn(II)	Mn(III)	Mn(IV)
Mn1	**1.98**	1.84	1.77
Mn2	3.38	**3.22**	3.16

Table S5. Bond valence sum calculations for **5**. The oxidation state for each metal is the whole number closest to the value in bold.

Atoms	Mn(II)	Mn(III)	Mn(IV)
Mn1	**1.99**	1.83	1.80
Mn2	**1.98**	1.84	1.81

Mn3	3.55	**3.24**	3.18
Mn4	4.23	3.92	**3.90**
Mn5	**1.93**	1.81	1.76
Mn6	**1.89**	1.80	1.75

Table S6. Bond valence sum calculations for **6**. The oxidation state for each metal is the whole number closest to the value in bold.

Mn1-O1	1.898(2)	Mn3-O35	1.961(2)	Mn6-O17	1.845(3)	Mn8-O20	2.196(3)
Mn1-O6	1.916(2)	Mn3-O3	2.135(2)	Mn6-O10	1.899(2)	Mn8-N1	2.233(3)
Mn1-O11	1.921(2)	Mn3-O11	2.385(2)	Mn6-O34	1.954(3)	Mn9-O17	2.086(3)
Mn1-O4	1.932(3)	Mn4-O17	1.852(2)	Mn6-N3	2.062(3)	Mn9-O30	2.129(3)
Mn1-O2	2.120(3)	Mn4-O18	1.854(3)	Mn6-O23	2.216(3)	Mn9-O32	2.165(3)
Mn1-O8	2.432(3)	Mn4-O16	1.859(2)	Mn6-O13	2.227(3)	Mn9-N5	2.253(3)
Mn2-O1	1.885(2)	Mn4-O8	1.924(2)	Mn7-O16	1.839(2)	Mn9-O22	2.265(3)
Mn2-O12	1.925(3)	Mn4-O11	1.946(2)	Mn7-O11	1.907(2)	Mn9-O33	2.278(3)
Mn2-O8	1.933(2)	Mn4-O10	1.955(2)	Mn7-O19	1.952(3)	Mn10-O31	2.031(3)
Mn2-O9	1.963(3)	Mn5-O18	1.836(3)	Mn7-O27	1.976(3)	Mn10-O16	2.045(3)
Mn2-O5	2.120(3)	Mn5-O8	1.909(3)	Mn7-O15	2.209(3)	Mn10-O24	2.098(3)
Mn2-O10	2.390(3)	Mn5-O21	1.934(3)	Mn7-O20	2.230(3)	Mn10-O28	2.144(3)
Mn3-O1	1.879(3)	Mn5-O25	1.984(3)	Mn8-O18	2.030(2)	Mn10-O23	2.174(3)
Mn3-O14	1.908(3)	Mn5-O22	2.201(3)	Mn8-O29	2.062(3)		
Mn3-O10	1.944(2)	Mn5-O7	2.243(3)	Mn8-O26	2.121(3)		

Table S7. Selected bond lengths (Å) for complex **1**.

Mn1-O2	2.121(6)	Mn1-N5	2.307(7)	Mn2-O4	2.254(5)	Mn3-O7	2.211(4)
Mn1-O1	2.170(4)	Mn1-O5^{I}	2.317(5)	Mn2-O5	2.258(4)	Mn3-O1^{I}	2.229(4)
Mn1-O4	2.200(5)	Mn2-O3	2.162(5)	Mn2-O6^{I}	2.302(4)	Mn3-N4^{I}	2.356(6)
Mn1-O6	2.236(5)	Mn2-O7	2.172(4)	Mn2-N3	2.309(6)	Mn3-N6	2.364(6)
Mn1-O3	2.291(5)	Mn2-N7	2.249(6)	Mn3-O8	2.174(4)	Mn3-N1^{I}	2.406(6)

Table S8. Selected bond lengths (Å) for complex **2**. Symmetry transformation: (I) 2 - x, 1 - y, z.

Mn1-O4^{I}	2.217(4)	Mn2-O8	2.105(2)	Mn3-O11	2.1554(19)	Mn4-N4^{I}	2.226(2)
Mn1-O5^{I}	2.226(4)	Mn2-O7	2.1422(17)	Mn3-O3	2.237(3)		
Mn1-O6^{I}	2.227(3)	Mn2-O9	2.1808(17)	Mn3-N3	2.250(2)		
Mn1-O2	2.228(4)	Mn2-O3	2.210(3)	Mn4-O4^{I}	2.076(3)		
Mn1-O1	2.230(4)	Mn2-N2	2.245(2)	Mn4-O12	2.116(2)		
Mn1-O3	2.233(4)	Mn3-O4^{I}	2.099(3)	Mn4-O11	2.1351(19)		
Mn1-N1	2.390(4)	Mn3-O10	2.1209(19)	Mn4-O2	2.160(3)		
Mn2-O5^{I}	2.071(3)	Mn3-O9	2.1309(18)	Mn4-O7^{I}	2.1827(18)		

Table S9. Selected bond lengths (Å) for complex **3**. Symmetry transformation: (I) 1 - x, - y, 1 – z.

Mn1-O3^{I}	2.091(4)	Mn1-O2	2.181(4)	Mn2-O1	2.216(4)	Mn2-O1^{III}	2.216(4)
Mn1-O1	2.154(4)	Mn1-O2^{I}	2.231(4)	Mn2-O1^{I}	2.216(4)	Mn2-O1^{IV}	2.216(4)
Mn1-O1^{v}	2.159(4)	Mn1-N1	2.242(5)	Mn2-O1^{II}	2.216(4)	Mn2-O1^{V}	2.216(4)

Table S10. Selected bond lengths (Å) for complex **4**. Symmetry transformation: (I) $^{1}/_{2}$ + z, x, $^{1}/_{2}$ – y. (II) 1 – y, ½ + z, ½ - x. (III) 1 – x, 1 – y, - z. (IV) ½ - z, 1 – x, y – ½. (V) y, ½ - z, x – ½.

Mn1-O1	2.1133(16)	Mn1-N2	2.333(2)	Mn2-O5^{I}	1.9106(17)	Mn2-O4^{I}	2.2251(16)
Mn1-O4	2.1832(16)	Mn1-N1	2.4097(19)	Mn2-O7	1.9203(15)		
Mn1-O3	2.2496(16)	Mn1-O3^{I}	2.4524(15)	Mn2-O3^{I}	1.9392(16)		
Mn1-O2	2.2825(17)	Mn2-O1	1.8941(15)	Mn2-O6	2.1536(16)		

Table S11. Selected bond lengths (Å) for complex **5**. Symmetry transformation: (I) 1 - x, 2 - y, 1 – z.

Mn1-O4	2.165(5)	Mn2-O6	2.248(6)	Mn4-O11	1.845(5)	Mn5-O20	2.281(5)
Mn1-O3	2.178(5)	Mn2-O8	2.268(5)	Mn4-O12	1.846(5)	Mn5-O11	2.305(5)
Mn1-O1	2.208(5)	Mn2-O12	2.312(5)	Mn4-O20	1.965(6)	Mn5-N3	2.428(7)
Mn1-O2	2.235(6)	Mn2-N2	2.432(7)	Mn4-O15	1.965(5)	Mn6-O17	2.179(6)
Mn1-O11	2.285(5)	Mn3-O12	1.890(5)	Mn4-O8	1.966(5)	Mn6-O16	2.199(6)
Mn1-O8	2.385(5)	Mn3-O11	1.897(5)	Mn4-O5	1.969(5)	Mn6-O19	2.211(5)
Mn1-N1	2.411(7)	Mn3-O13	1.953(5)	Mn5-O14	2.179(5)	Mn6-O18	2.236(7)
Mn2-O9	2.167(6)	Mn3-O10	1.959(5)	Mn5-O21	2.199(6)	Mn6-O12	2.303(5)
Mn2-O7	2.207(6)	Mn3-O19	2.143(5)	Mn5-O19	2.255(5)	Mn6-O20	2.339(6)
Mn2-O3	2.234(5)	Mn3-O3	2.167(6)	Mn5-O22	2.259(6)	Mn6-N4	2.446(8)

Table S12. Selected bond lengths (Å) for complex **6**.

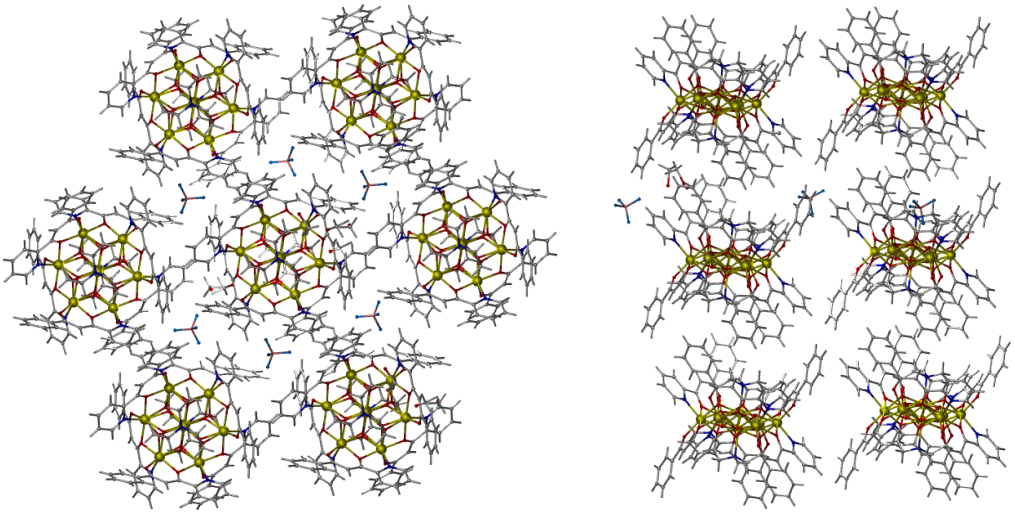

Figure S1. Hexagonal packing arrangement of **3** (left) and stacked layers (right).

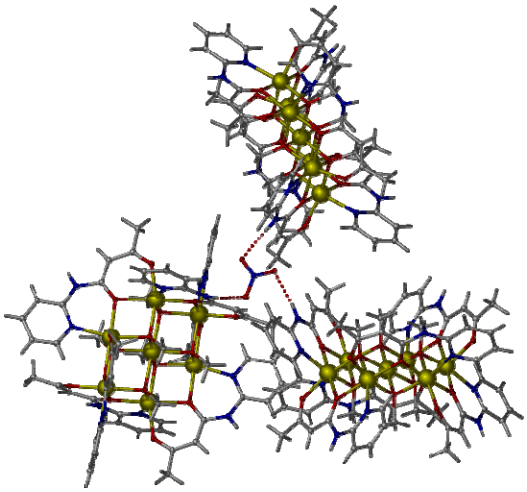

Figure S2. Crystal packing in **4**, displaying the triply H-bonded nitrate. H-bonds shown as dashed lines.

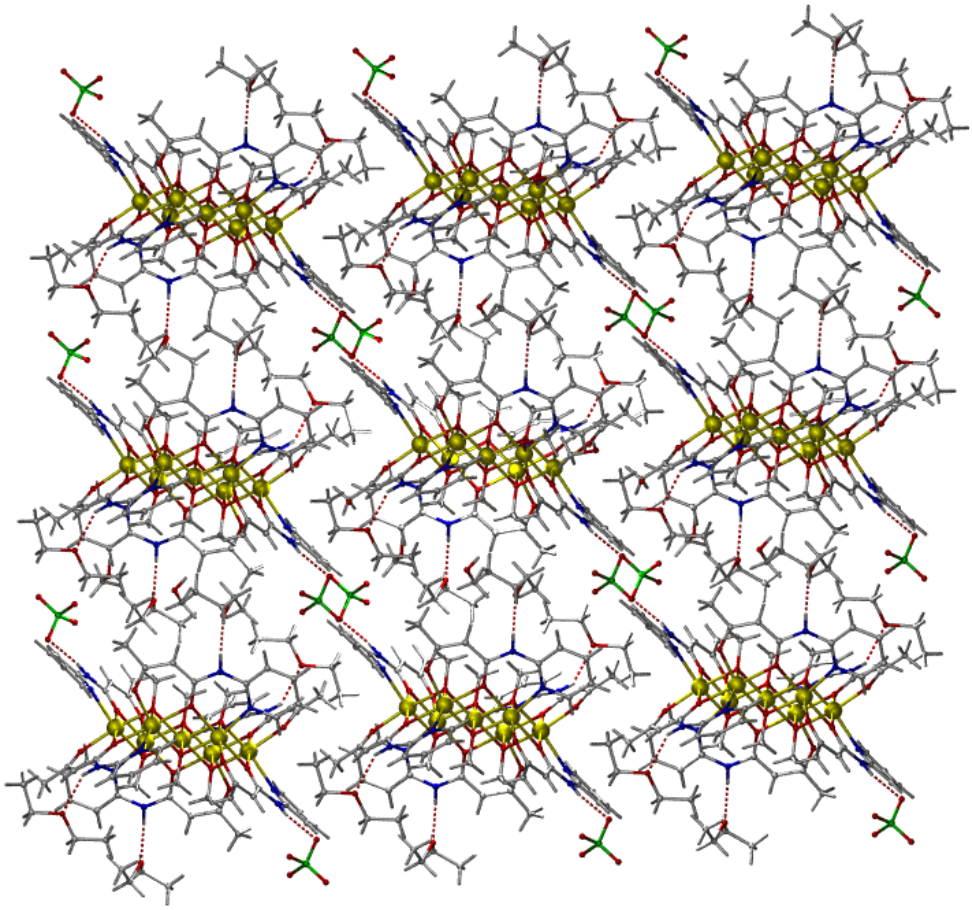

Figure S3. Crystal packing in **4a**. H-bonds shown as dashed lines.

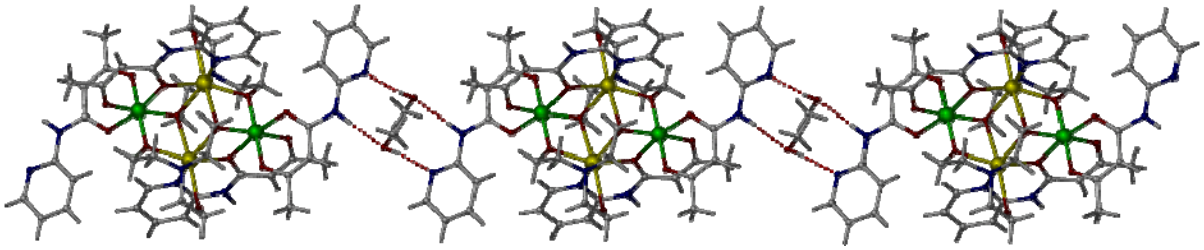

Figure S4. 1-D hydrogen bonded chains formed between the pyridyl ring, methanol solvent molecule and the NH group from the secondary amine, in **5**. Dashed lines indicate the H-bonds.

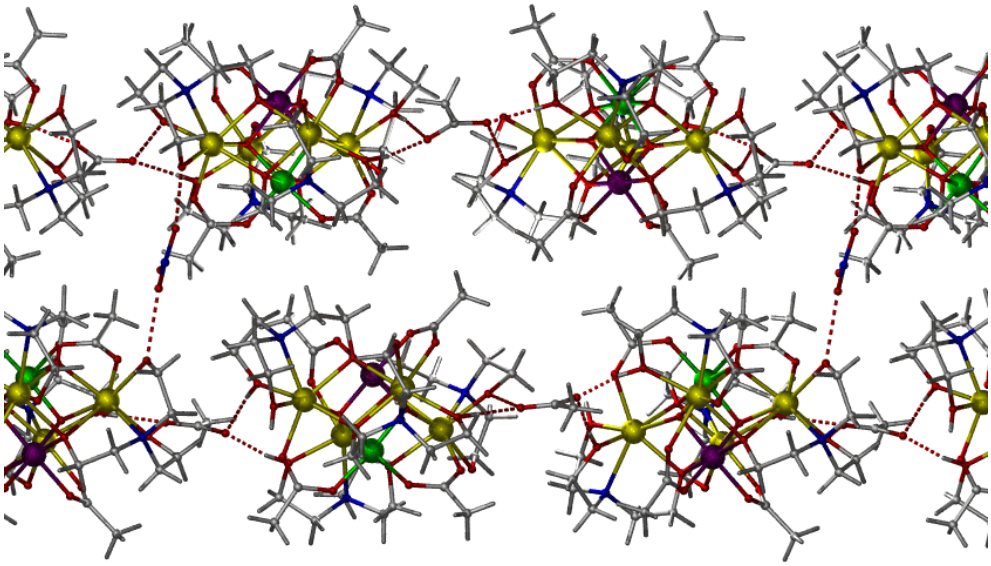

Figure S5. 2-D hydrogen bonded sheets formed between the $teaH_2^-$, acetate and the nitrate group, in **6**. Dashed lines indicate the H-bonds.

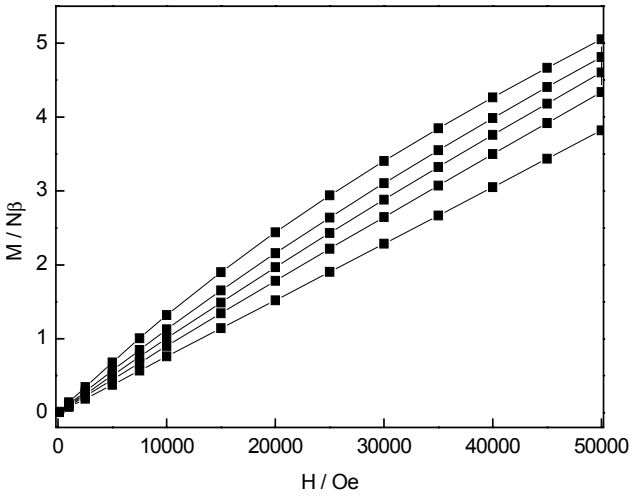

Figure S6. *M* vs *H* isothermal plots for **1** in the 2 (top) – 20 K (bottom) temperature range (right), the solid lines are guides for the eye.

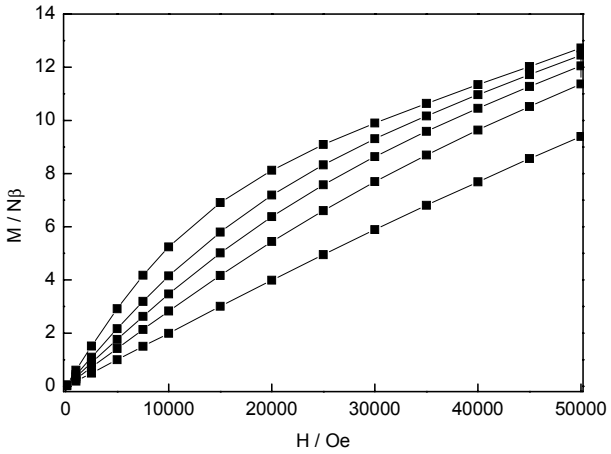

Figure S7. *M* vs *H* isothermal plots for **2** in the 2 (top) – 20 K (bottom) temperature range (right), the solid lines are guides for the eye.

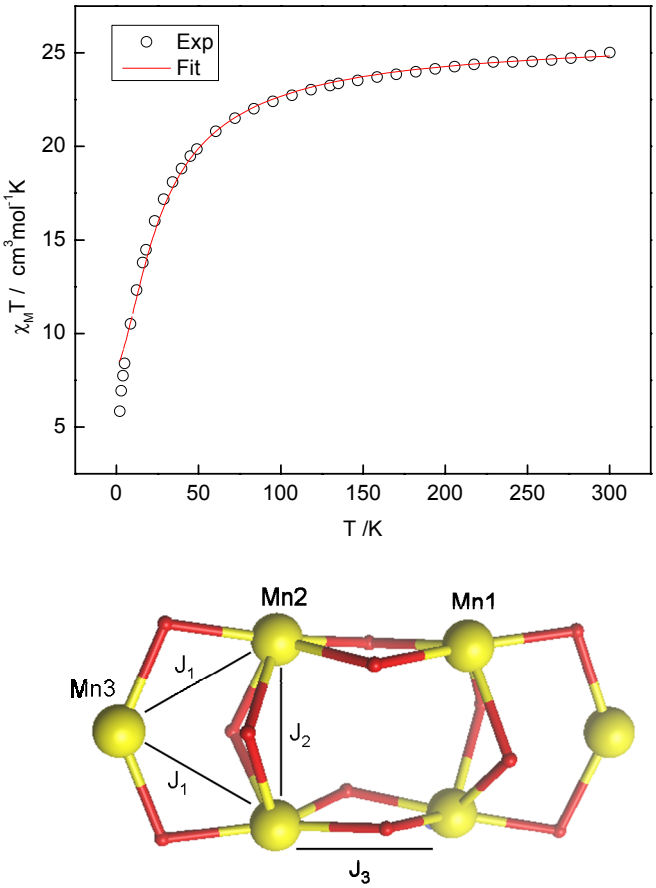

Figure S8. Fit for **2** (above) using the coupling scheme shown (below).

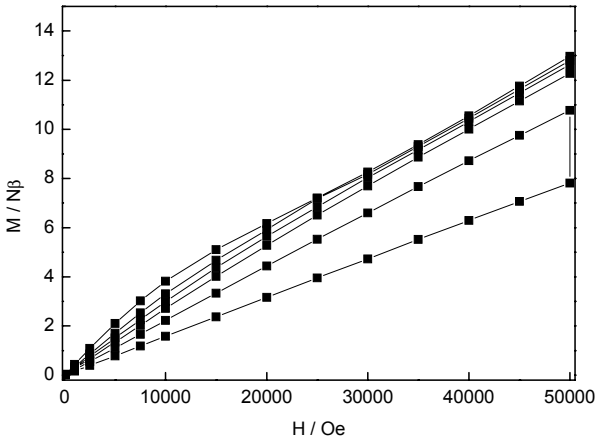

Figure S9. *M* vs *H* isothermal plots for **3** in the 2 (top) – 20 K (bottom) temperature range (right), the solid lines are guides for the eye.

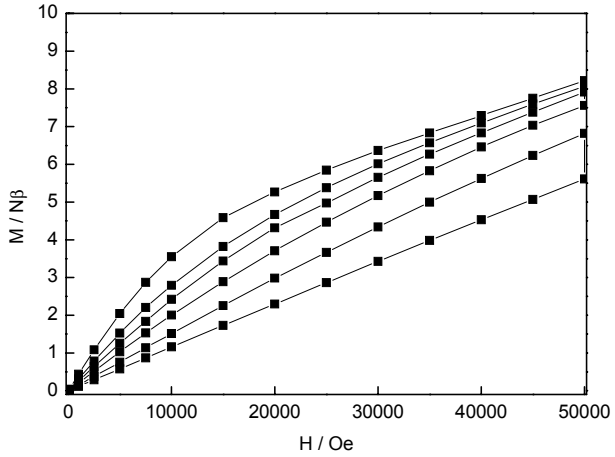

Figure S10. *M* vs *H* isothermal plots for **4** in the 2 (top) – 20 K (bottom) temperature range (right), the solid lines are guides for the eye.

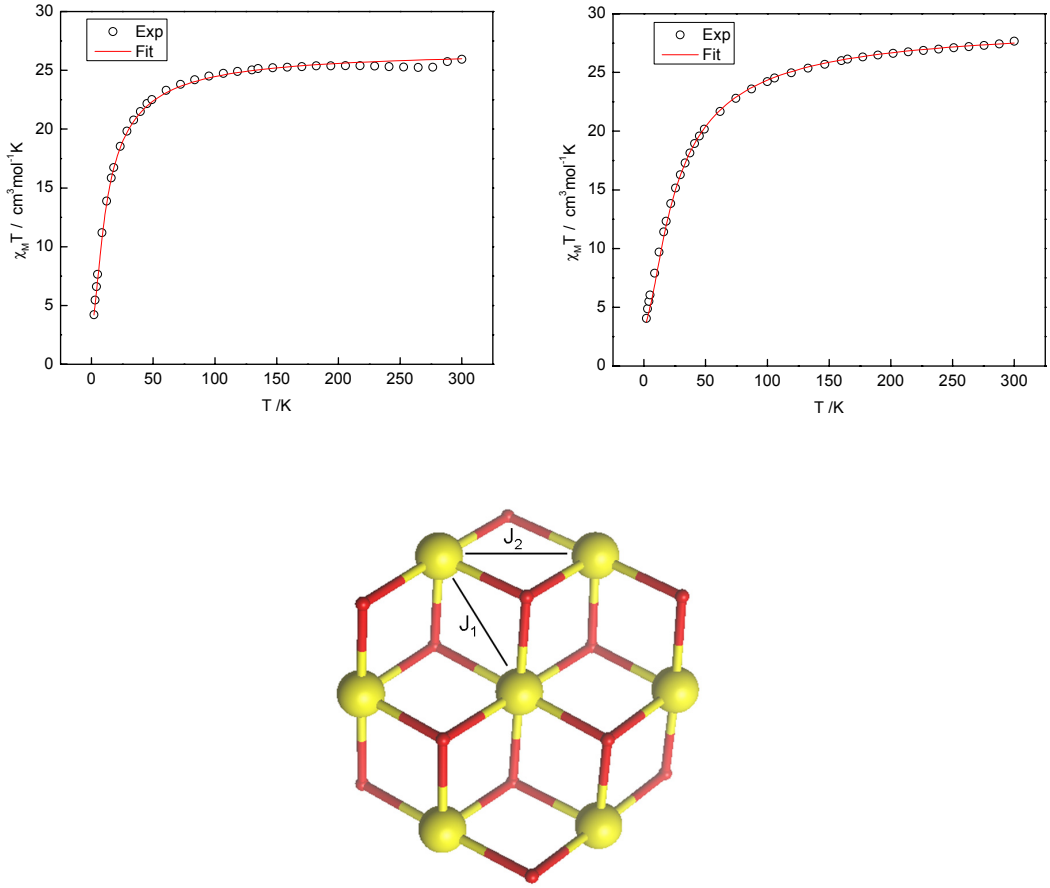

Figure S11. Fits for **3** (above left) and **4** (above right) using the coupling scheme shown (below). Each centre to ring (J_1) and ring to ring (J_2) interaction are assumed to be equal.

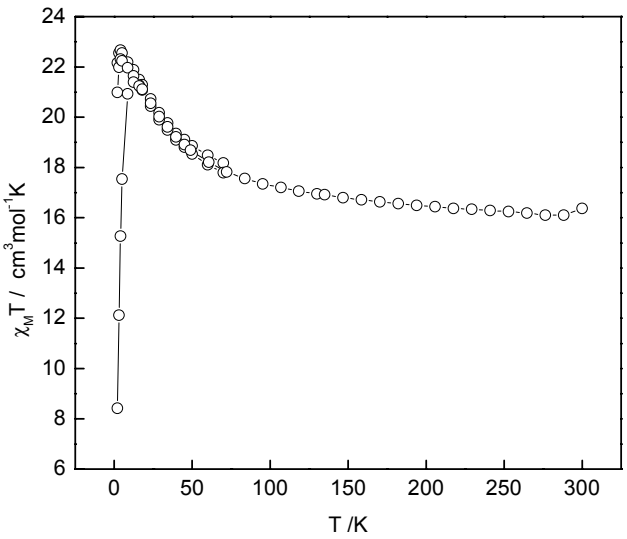

Figure S12. $\chi_M T$ versus T plot for **5** in DC fields of 1 (bottom; range 2 – 300 K) and 0.1 and 0.01 T (top) in the range of 2 – 70 K.

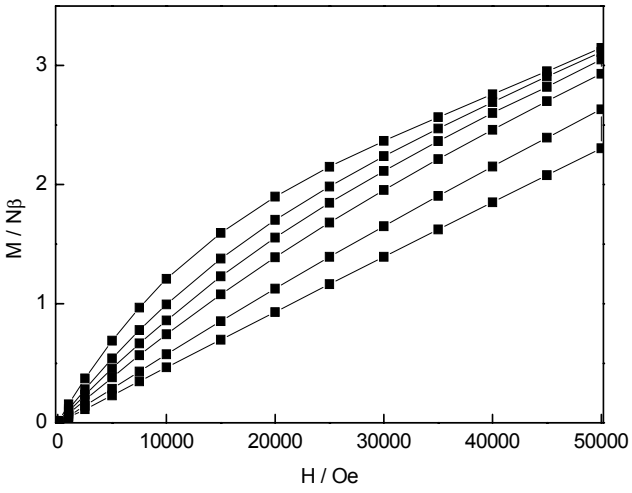

Figure S13. *M* vs *H* isothermal plots for **6** in the 2 (top) – 20 K (bottom) temperature range (right), the solid lines are guides for the eye.

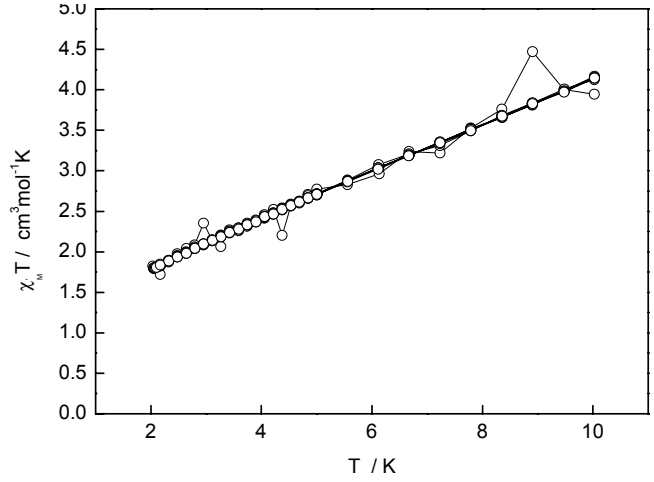

Figure S14. Plot of $\chi_M' T$ vs. *T* for **1** in AC frequencies 2000 - 250 Hz.

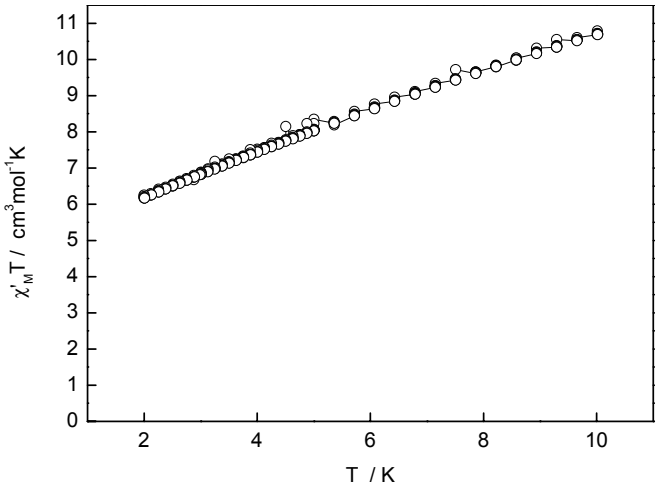

Figure S15. Plot of $\chi_M' T$ vs. *T* for **2** in AC frequencies 2000 - 250 Hz.

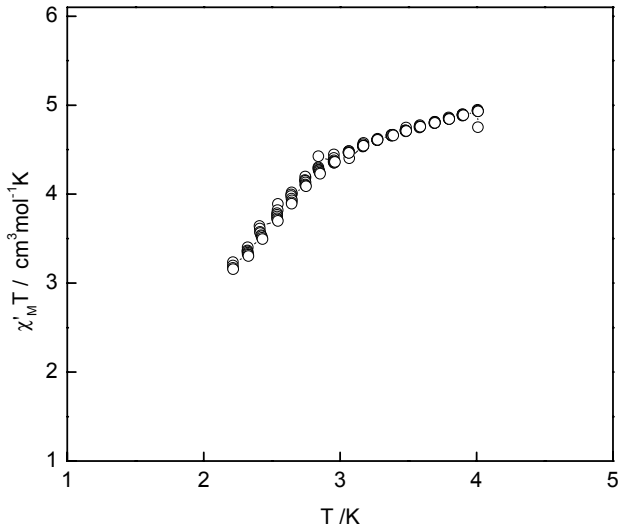

Figure S16. Plot of $\chi_M{}' T$ vs. T for **3** in AC frequencies 2000 - 250 Hz.

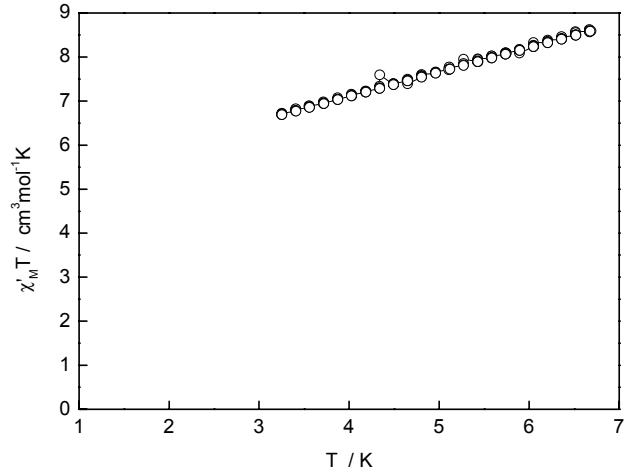

Figure S17. Plot of $\chi_M{}' T$ vs. T for **4** in AC frequencies 2000 - 250 Hz.

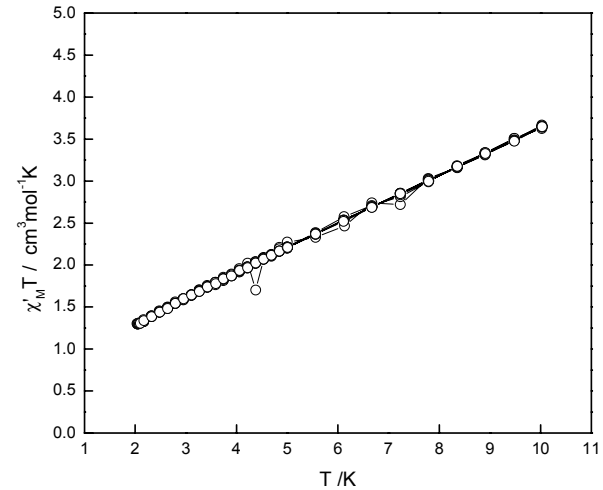

Figure S18. Plot of $\chi_M{}' T$ vs. T for **6** in AC frequencies 2000 - 250 Hz.